

Aleksandra S. Popović<sup>1,\*</sup>, Dušan Vujošević<sup>1</sup>, Milan Milivojević<sup>1</sup>, Tomislav Trišović<sup>2</sup>, Lazar Rakočević<sup>3</sup>, Branimir N. Grgur<sup>1</sup>

<sup>1</sup>Department of Physical Chemistry and Electrochemistry, University of Belgrade Faculty of Technology and Metallurgy, Belgrade, Serbia,

<sup>2</sup>Institute of Technical Sciences of SASA, Belgrade, Serbia, <sup>3</sup>INS Vinča, Department of Atomic Physics, University of Belgrade, Belgrade, Serbia

Scientific paper

ISSN 0351-9465, E-ISSN 2466-2585

<https://doi.org/10.62638/ZasMat1328>



Zastita Materijala 66 (4)  
880 - 886 (2025)

## The influence of the tartarate on the deposition-dissolution of zinc for the application in aqueous battery

### ABSTRACT

Zinc-ion batteries (ZIBs) have recently gained significant attention as a sustainable energy storage solution due to their cost-effectiveness and safety. Despite offering high theoretical capacity and low redox potential, ZIBs face challenges such as dendrite growth and low zinc utilization rates, which hinder their performance. The objective of this study was to optimize the electrolyte composition to enhance the performance of a zinc electrode electrochemically deposited on a copper substrate within the zinc(II)-NH<sub>4</sub>Cl system. The influence of Zn<sup>2+</sup> and NH<sub>4</sub><sup>+</sup> ion concentrations, current density, and the addition of sodium tartrate on the morphology and behavior of the anode material during charge and discharge cycles was examined. Results demonstrated that the addition of sodium tartrate significantly improves the electrochemical performance of the anode material and reduces corrosion in the electrolyte. The findings from this study suggest that electrolyte engineering could potentially provide a solution for better performance and extended longevity of ZIBs.

**Keywords:** Zinc-ion batteries, sodium tartrate, additive, anode, corrosion.

### 1. INTRODUCTION

The two-electron redox capability of zinc, offering a notable energy density of 820 mAh g<sup>-1</sup> and 5851 mAh cm<sup>-3</sup>, combined with the cost-effectiveness and widespread availability of zinc metal, establishes zinc-ion batteries (ZIB's) as promising candidates for large-scale energy storage applications [1–3]. The zinc anode offers low toxicity and remarkable stability across diverse aqueous electrolytes, largely attributed to a significant overpotential for hydrogen evolution despite its relatively low redox potential of -0.76 V vs. SHE [2,4,5]. This compatibility with a broad array of cathode materials has intensified research interest in ZIB's as highly suitable for grid-scale energy storage [1,3,4,6]. Among, vanadium-based compounds, Prussian blue analogs, MXene and its composites, and different organic materials, the manganese dioxide, MnO<sub>2</sub>, with different structures is most widely investigated and shows very good electrochemical characteristics for zinc intercalation/deintercalation in near-neutral aqueous electrolytes including chloride based [7, 8].

Manganese is abundant, readily available, low cost, environmentally friendly, and MnO<sub>2</sub> can be easily synthesized. Additionally, manganese has a high voltage plateau (1.2–1.4 V) revealing a high energy density and exists variety of oxidation states including Mn<sup>2+</sup>, Mn<sup>3+</sup>, Mn<sup>4+</sup>, and Mn<sup>7+</sup>[7].

Aqueous electrolytes are increasingly recognized as optimal for ZIB's due to their safety, affordability, and environmental advantages [4]. Utilizing zinc anodes and water-based electrolytes, ZIB's offer high ionic conductivity, enabling rapid charge and discharge [6–9]. However, these systems face persistent challenges, such as dendrite formation, corrosion, and suboptimal electrode-electrolyte interfaces, all of which affect their durability and efficiency [10–13]. Zinc's charge storage mechanism involves a reversible Zn plating/stripping cycle in aqueous electrolytes, where, upon charging, Zn<sup>2+</sup> ions are reduced and deposited onto the Zn anode. Conversely, during discharge, zinc is oxidizing into Zn<sup>2+</sup> ions. Dendrite formation is primarily driven by irregular Zn ion flux and an uneven electric field during reversible cycling, which can lead to larger dendrites that penetrate the separator, potentially causing short circuits [2,10,12,13]. Additionally, these structures increase the surface area of the Zn anode, intensifying side reactions such as corrosion and hydrogen evolution [6,14].

\*Corresponding author: Aleksandra S. Popović

E-mail: apopovic@tmf.bg.ac.rs

Paper received: 24.12.2024.

Paper accepted: 24.01.2025.

To address these limitations, a range of strategies has been explored, including protective coatings for the zinc anode, modification of zinc deposition's crystallographic orientation, three-dimensional Zn architectures, alloying with inert metals, and electrolyte optimization [2,10-12]. A holistic approach appears to lie in electrolyte engineering, focusing on high-concentration electrolytes and additive incorporation to fine-tune the solvation structure of  $Zn^{2+}$  ions [11,12,16-19]. This technique substantially impacts nucleation processes, inhibiting dendrite growth and reducing unwanted side reactions. Specifically, various additives such as polyethylene oxide (PEO), polyethylene glycol (PEG), polyacrylamide (PAM), methanol, and dimethyl sulfoxide (DMSO) effectively modulate the  $Zn^{2+}$  solvation shell [1,11]. These additives limit 2D zinc ion diffusion, enabling even current distribution and fostering uniform zinc deposition [1,12].

The objective of this study was to enhance the performance of a zinc electrode electrochemically deposited on a copper substrate within the zinc(II)- $NH_4Cl$  system. The influence of  $Zn^{2+}$  and  $NH_4^+$  ion concentrations, current density, and the addition of Na-tartarate on the morphology and behavior of the anode material during charge and discharge cycles was examined. Results demonstrated that the addition of Na-tartrate improved capacity retention during cycling and reduced charge/discharge overpotentials. Furthermore, corrosion testing revealed that the corrosion rate in the solution with the additive was decreased.

## 2. EXPERIMENTAL

Zinc plating/stripping behavior was investigated in the electrolyte consisting of zinc chloride, which concentration was kept constant, 0.5 M, and varying the ammonium chloride electrolytes in the range of 0 to 2 M, along with the addition of 20 mM Na-tartarate additive. Solutions were prepared from p.a. grade chemicals (Merck). The concentration of Na-tartarate was selected based on literature data suggesting a suspensive nature and recrystallization of the solute (Zn-tartarate) [16]. In order to investigate the kinetics of the deposition/dissolution reaction, and determine the optimal electrolyte, the behavior of pure zinc plates (Alfa Aesar) was examined in the investigated solutions by recording galvanodynamic curves from  $5 \mu A \text{ cm}^{-2}$  to  $80 \text{ mA cm}^{-2}$  in both anodic and cathodic directions. The open circuit potential (OCP) was measured before the scan, scanning began with OCP in the more negative direction, swept back to near the OCP potential.

The influence of  $NH_4Cl$  concentration on zinc deposition/dissolution was investigated on the pure copper plate (10 mm x 10 mm x 0.5 mm,  $S = 2$

$\text{cm}^2$ ). Before use, copper plates were treated by dipping into an 8MHNO<sub>3</sub> solution for 10 seconds, washed with deionized water, and dried in the air. Zinc deposition/dissolution was investigated by cyclic voltammetry curves using a scan rate of 5 mVs<sup>-1</sup>. The influence of the ammonium chloride concentration on cathodic and anodic overpotentials was investigated by recording galvanostatic curves at the constant current density of  $j = 50 \text{ mA cm}^{-2}$  and constant deposition charge of  $q = 10 \text{ mAh cm}^{-2}$ . The optimal electrolyte was found to be, 0.5 M  $ZnCl_2$  and 1 M  $NH_4Cl$ , in which the influence of deposition/dissolution current densities, in the range of  $20 \text{ mA cm}^{-2}$  to  $50 \text{ mA cm}^{-2}$ , on the current efficiency was investigated, without and with the addition of 20 mM Na-tartarate.

The morphology of the deposits was investigated from the optimal electrolyte, 0.5 M  $ZnCl_2$ , and 1 M  $NH_4Cl$ , without and with the addition of 20 mM Na-tartarate, by applying a current density of  $j=50 \text{ mA cm}^{-2}$  over 1h. Cyclic behavior was investigated with a current density of  $50 \text{ mA cm}^{-2}$  over 100 cycles.

All the experiments were performed in a three-compartment glass cell with 100 mL of electrolyte solution, using the zinc plate as a counter electrode, and saturated calomel electrode as a reference electrode.

To evaluate self-discharge impact, the corrosion behavior of zinc deposits electrochemically synthesized on copper plates ( $j=50 \text{ mA cm}^{-2}$ , 1h) was examined by immersing them in the solution of 0.5 M  $ZnCl_2$  and 1 M  $NH_4Cl$ , 100 mL, with and without Na-tartrate for 7 days. The corrosion current density was determined by measuring the masses of the plates before and after immersion in the solutions and applying Faraday's law. The morphology of the deposits, before and after the corrosion test, was examined by optical microscopy. All measurements were performed using a potentiostat/galvanostat Gamry 1010E, while micrographs were obtained using the optical microscope Olympus CX41 connected to the PC.

## 3. RESULTS AND DISCUSSION

Figure 1 shows galvanodynamic polarization curves of the zinc chloride,  $ZnCl_2$  with the addition of different concentrations of ammonium chloride,  $NH_4Cl$  on the solid zinc electrode. Because Tafel behavior is not observed, the slope is below 10 mV dec<sup>-1</sup>, it could be concluded that reactions of the zinc deposition and dissolution are under mixed diffusion-activation control, as also suggested by Cao et al. [20]. From the inset in Fig. 1, it can be clearly seen that diffusion is dominant even near the reversible potential because the mixing of the solutions influences the polarization curve. For such a case the dependence of current on potential can be expressed by the following equation [21]:

$$j = \left\{ \frac{\left\{ j_0 \exp \left[ \frac{2.3(E-E_r)}{b_a} \right] \right\}^\gamma}{1 + \left\{ \frac{j_0}{j_{d,a}} \exp \left[ \frac{2.3(E-E_r)}{b_a} \right] \right\}^\gamma} - \frac{\left\{ j_0 \exp \left[ -\frac{2.3(E-E_r)}{b_c} \right] \right\}^\gamma}{1 + \left\{ \frac{j_0}{j_{d,c}} \exp \left[ -\frac{2.3(E-E_r)}{b_c} \right] \right\}^\gamma} \right\}^\frac{1}{\gamma}$$

where  $j_0$  is exchange current density,  $j_d$  limiting diffusion current density,  $E_r$  reversible electrode potential,  $E$  actual potential, and,  $\gamma$  is an integer curvature-defining constant, controlling the sharpness of the curve in the transition from the activation-controlled to the diffusion-controlled currents, and can have the value of 2 to 4.

From Fig. 1 can be seen that at constant potential, current increases with the addition of ammonium chloride. This could be explained by the formation of zinc chloride complex that has a higher value of the diffusion coefficient. Namely, at low chloride concentrations the dominant species is hydrated  $Zn^{2+}$ , while with the addition of chloride the dominant species become  $ZnCl_4^{2-}$  [22]. The formation of zinc chloride ammonium complexes is favored at higher pH [23].

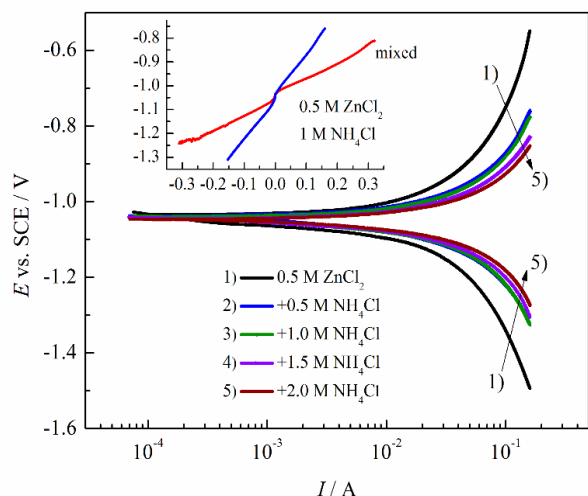


Figure 1. Galvanodynamic polarization curves ( $v = 100 \mu A s^{-1}$ ) of zinc deposition and dissolution on solid zinc electrode ( $S = 2 cm^2$ ) with different ammonium chloride concentrations (marked in the figure). Inset: polarization curves without and with the mixing of the solution

A similar observation can be seen from the cyclic voltammetry experiments shown in Fig. 2. Without ammonium chloride in the solution, for cathodic potential limits of  $-1.25$  V current is  $\sim 50$  mA, while with the addition of ammonium chloride current increase. Also, the anodic zinc stripping peak is shifted to more negative potentials with an increase in chloride concentrations, and the charge associated with zinc is much higher than in a pure  $ZnCl_2$  solution. This confirms that  $ZnCl_4^{2-}$  can be much more easily reduced than hydrated  $Zn^{2+}$  ions in the form of  $[Zn(H_2O)_6]^{2+}$  which is very stable

[24]. A similar effect is observed by the addition of the N-Methylmethanesulfonamide (NMS) to optimize the transfer, dehydration, and reduction of  $Zn^{2+}$  [25].

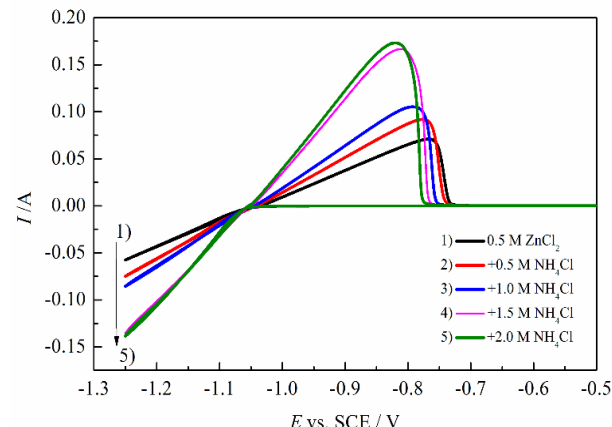


Figure 2. Cyclic voltammograms ( $v = 5 mV s^{-1}$ ) of zinc deposition and dissolution on the solid copper electrode ( $S = 2 cm^2$ ) with different ammonium chloride concentrations (marked in the figure)

To determine the influence of the chloride concentration on the overpotentials for the deposition/dissolution reaction of zinc, Fig. 3, the zinc is deposited for 1800 s, and dissolve with a current density of  $50 \text{ mA cm}^{-2}$ .

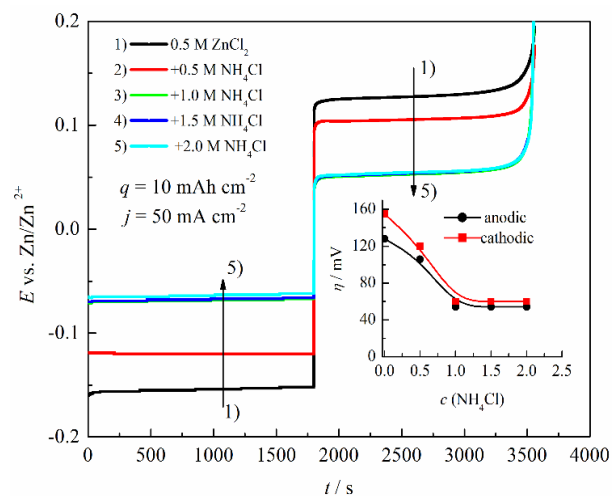


Figure 3. The influence of the ammonium chloride concentration on the overpotentials for deposition/dissolution reaction of zinc on copper electrode ( $S = 2 cm^2$ ). Inset: The dependence of overpotentials for zinc deposition/dissolution for different ammonium chloride concentrations

From the inset in Fig. 3, it can be seen that with increasing chloride concentration, both deposition and dissolution overpotentials significantly decrease, up to the ammonium chloride concentration of 1 M, when it is stabilized. Therefore, the excess of chloride concentrations is necessary to reduce deposition and dissolution overpotentials.

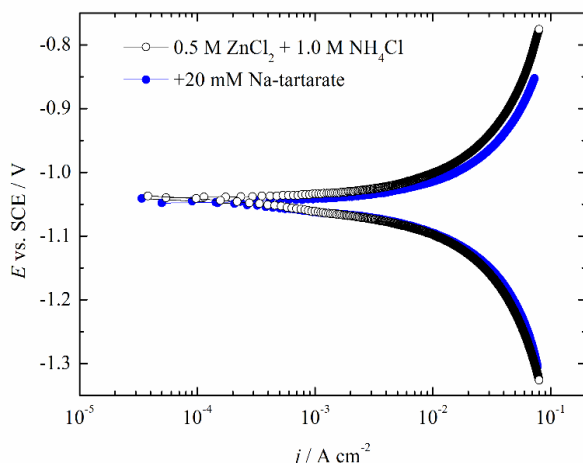


Figure 4. Galvanodynamic polarization curve ( $v = 100 \mu\text{A s}^{-1}$ ) on solid zinc electrode without and with the addition of 20 mM Na-tartarate

Based on the above given results, for the following investigations electrolyte based on 0.5 M

$\text{ZnCl}_2$  and 1.0 M  $\text{NH}_4\text{Cl}$  is chosen. Also, the influence of tartarate addition is investigated. Figure 4 shows the galvanodynamic polarization curve on a solid zinc electrode without and with the addition of 20 mM Na-tartarate. Some slight increase in current density is observed with the addition of tartarate.

In order to investigate the influence of tartarate addition on the current efficiency the deposition/dissolution is investigated by applying different current densities on the copper electrode, in the range from 20 to 50  $\text{mA cm}^{-2}$  using the following equation:

$$\eta = \frac{t_d}{t_c} \times 100$$

Where:  $t_d$  is discharge time, and  $t_c$  is charge time.

From the insets of Figs. 5a and 5b, it can be seen that in the electrolyte without the addition of tartarate, at lower current densities, e.g. 20  $\text{mA cm}^{-2}$  current efficiency is 85% and gradually increases with applied currents up to 97%. On the contrary, with the addition of tartarate, at low current density, efficiency is significantly higher, 95%, and increases to 100% for higher current densities.

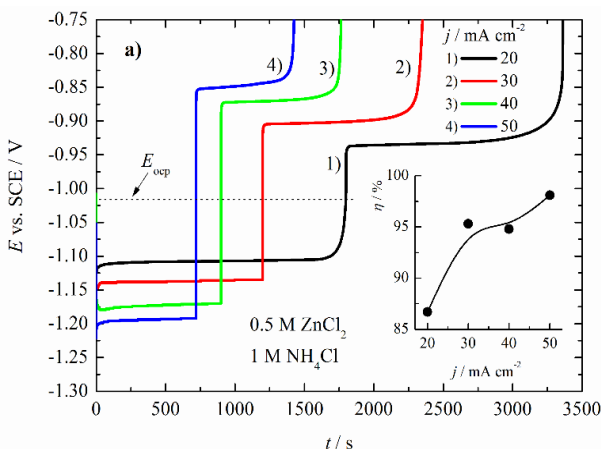
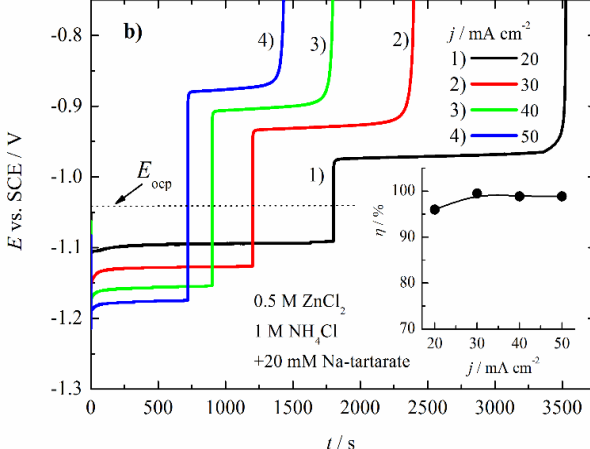


Figure 5. Galvanostatic curve for deposition and dissolution of the zinc on the copper electrode a) without tartarate, and b) with the addition of 20 mM Na-tartarate. Insets: Current efficiency of zinc electrodeposition

Such behavior could be explained based on Figs. 6a and 6b where optical micrographs of the electrodeposited zinc without and with tartarate for a deposition charge of 50  $\text{mA h cm}^{-2}$  are shown. It is obvious that without tartarate in the solution throwing power is much lower than with tartarate, and some uncovered copper can be seen. Hence, initially, without tartarate on the copper electrode much more hydrogen is evolved decreasing current



efficiency. It could be postulated that tartarates are adsorbed on the energetically more active sites and partially block hydrogen evolution reaction. Also, from Fig. 6, it can be seen that with tartarate in the solution, more homogeneous deposits are obtained which can be explained by the same postulation, by the blocking effects of the active sites on which inhomogeneous deposition can occur.

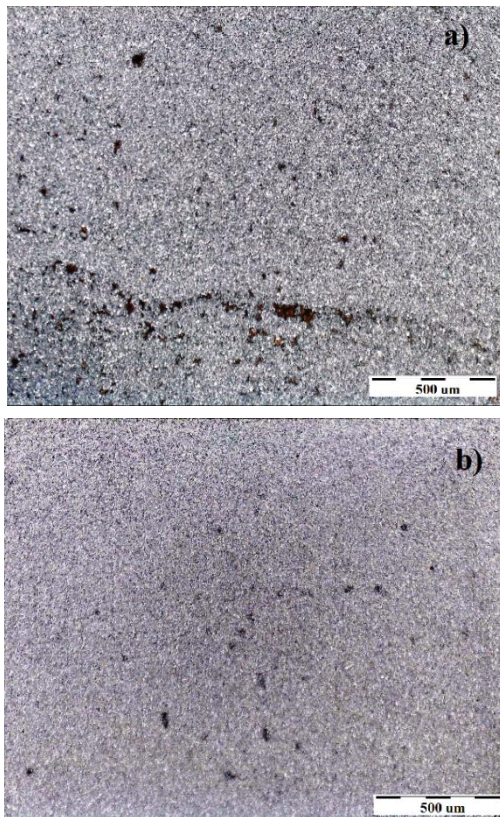


Figure 6. The optical micrographs of the zinc deposits on copper electrode a) without and b) with 20 mM Na-tartarate, were obtained at a deposition current density of 50 mA cm<sup>-2</sup> during 1 h.

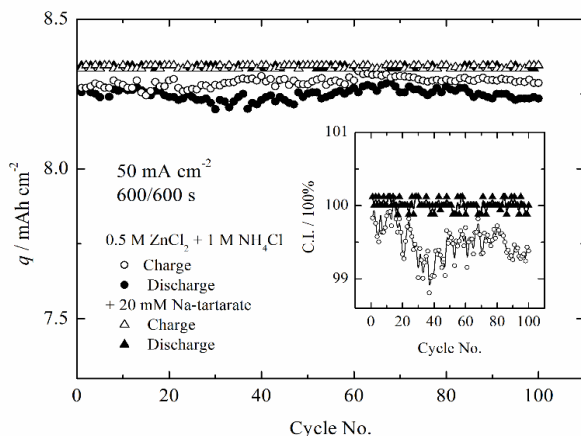


Figure 7. Cyclization behavior of Zn on the copper plate during 100 cycles, 600 s charge, and 600 s discharge in the solution of 0.5 M ZnCl<sub>2</sub> and 1 M NH<sub>4</sub>Cl without tartarate, and with the addition of 20 mM Na-tartarate. Inset: Coulombic efficiency of zinc deposition/dissolution

Figure 7 shows the cyclization behavior of Zn on the copper plate during 100 cycles, with 600 s charge, and 600 s discharge in the solution of 0.5 M ZnCl<sub>2</sub> and 1 M NH<sub>4</sub>Cl, without tartarate and with the addition of 20 mM Na-tartarate, by applying the current density of 50 mA cm<sup>-2</sup>. It can be seen that

with the addition of Na-tartarate, charge/discharge is much more uniform, than without tartarate. From the inset in Fig.7, where Coulombic efficiency (C.I.) of zinc deposition/dissolution is shown, it can be concluded that both systems have high current efficiency, but without tartarate C.I. is more scattered.

To evaluate the corrosion behavior of zinc deposits electrochemically synthesized on the copper plates,  $j=50$  mA cm<sup>-2</sup> during 1 h, is examined by immersing them in two investigated solutions, without and with 20 mM Na-tartarate for 7 days, and results are shown in Table 1. The corrosion current density is calculated using the following equation:

$$j_{corr} = \frac{\Delta m M(Zn)}{S t n F}$$

Here  $\Delta m$  is mass change, S surface area of 2 cm<sup>2</sup>,  $t = 168$  h, and  $F = 26.8$  Ah mol<sup>-1</sup>.

Table 1. Copper mass before and after zinc corrosion test in the investigated solutions and calculated corrosion current density

c(Na-tar.)/mM	$m_1/g$	$m_2/g$	$\Delta m/g$	$j_{corr}/\mu A cm^{-2}$
0	0.3677	0.3584	0.0103	37.4
20	0.3710	0.3682	0.0028	10.2

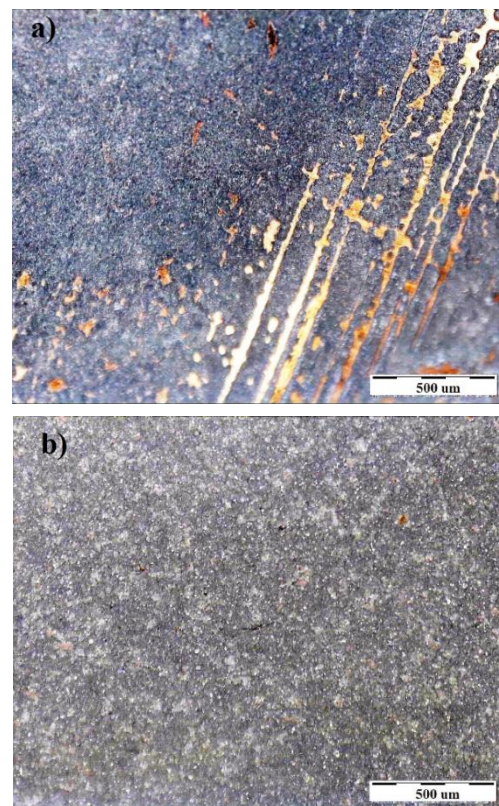


Figure 8. The optical micrographs of the zinc deposits on copper electrode after 7 days of exposure to the corrosion solution. a) without and b) with 20 mM Na-tartarate, obtained at a deposition current density of 50 mA cm<sup>-2</sup> during 1 h

From the calculated corrosion current density, it is obvious that in the presence of tartarate corrosion is almost four times smaller than in the solution with tartarate. From Figs. 8a) and 8b) it is obvious that without tartarate in the solution, a high area of copper is visible. This could be explained that tartarate is adsorbed on active sites for hydrogen evolution, acting as corrosion inhibitor.

#### 4. CONCLUSIONS

The paper analyzes the influence of electrolyte composition on the electrochemical behavior of the zinc anode electrochemically deposited on a copper substrate in the Zn(II)-NH<sub>4</sub>Cl system. The results demonstrate a significant effect of electrolyte composition on the performance of the zinc-ion battery anode. Galvanodynamic polarization studies reveal that zinc deposition and dissolution in the NH<sub>4</sub>Cl-ZnCl<sub>2</sub> system occur under mixed diffusion-activation control. The addition of ammonium chloride enhances current density, which is attributed to the formation of ZnCl<sub>4</sub><sup>2-</sup> complexes with higher diffusion coefficient. Increasing chloride concentrations leads to a reduction in both deposition and dissolution overpotentials, with stabilization observed at 1 M ammonium chloride. Furthermore, the incorporation of sodium tartrate significantly improves deposition uniformity, likely by adsorbing onto active sites and inhibiting hydrogen evolution, which results in reduced corrosion and improved current efficiency. These findings underscore the critical role of additives in optimizing the performance of zinc-ion battery anodes.

The future work will be focused on synthesis of MnO<sub>2</sub> positive active materials, and investigation of his electrochemical behavior, as a single electrode and in combination with zinc negative electrode in the optimal electrolyte.

#### Financing

*This study was supported by the Ministry of Education, Science and Technological Development, grant number: 451-03-65/2024-03/200135*

#### 5. REFERENCES

- [1] Q. Meng, T. Yan, Y. Wang, X. Lu, H. Zhou, S. Dong (2024) Critical design strategy of electrolyte engineering toward aqueous zinc-ion battery, *Chemical Engineering Journal*, 497, 154541. <https://doi.org/10.1016/j.cej.2024.154541>
- [2] J. Hao, X. Li, X. Zeng, D. Li, J. Mao, Z. Guo (2020) Deeply understanding the Zn anode behaviour and corresponding improvement strategies in different aqueous Zn-based batteries, *Energy & Environmental Science* 13(11), 3917-3949. <https://doi.org/10.1039/D0EE02162H>
- [3] Y. Su, X. Wang, S. Zhou, X. Zou, H. Sun, D. Liu, G. Zhu (2022) A specific free-volume network as synergistic zinc-ion-conductor interface towards stable zinc anode, *Energy Storage Materials*, 53, 909-916. <https://doi.org/10.1016/j.ensm.2022.10.016>
- [4] Z. Hu, F. Zhang, A. Zhou, X. Hu, Q. Yan, Y. Liu, F. Arshad, Z. Li, R. Chen, F. Wu, L. Li (2023) Highly reversible Zn metal anodes enabled by increased nucleation overpotential, *Nano-Micro Letters*, 15(1), 171. <https://doi.org/10.1007/s40820-023-01136-z>
- [5] H. Yan, S. Li, J. Zhong, B. Li (2024). An electrochemical perspective of aqueous zinc metal anode, *Nano-Micro Letters*, 16(1), 15. <https://doi.org/10.1007/s40820-023-01227-x>
- [6] G. Fang, J. Zhou, A. Pan, S. Liang (2018) Recent advances in aqueous zinc-ion batteries, *ACS Energy Letters*, 3(10), 2480-2501. <https://doi.org/10.1021/acsenergylett.8b01426>
- [7] X. Zhou, S. Jiang, S. Zhu, S. Xiang, Z. Zhang, X. Xu, Y. Xu, J. Zhou, S. Tan, Z. Pan, X. Rao, Y. Wu, Z. Wang, X. Liu, Y. Zhang, Y. Zhou (2023) The progress of cathode materials in aqueous zinc-ion batteries. *Nanotechnology Reviews*, 12(1), 20230122. <https://doi.org/10.1515/ntrev-2023-0122>
- [8] N. J. Herrmann, B. Horstmann (2024) Model-based electrolyte design for near-neutral aqueous zinc batteries with manganese-oxide cathodes, *Energy Storage Materials*, 70, 103437. <https://doi.org/10.1016/j.ensm.2024.103437>
- [9] P. Yu, Y. Zeng, H. Zhang, M. Yu, Y. Tong, X. Lu (2019) Flexible Zn-ion batteries: recent progresses and challenges, *Small*, 15(7), 1804760. <https://doi.org/10.1002/smll.201804760>
- [10] S. Guo, L. Qin, T. Zhang, M. Zhou, J. Zhou, G. Fang, S. Liang (2021) Fundamentals and perspectives of electrolyte additives for aqueous zinc-ion batteries, *Energy Storage Materials*, 34, 545-562. <https://doi.org/10.1016/j.ensm.2020.10.019>
- [11] Y. Zhou, X. Ni, B. Hao, X. Zhou, C. Yan, J. Zhou, T. Qian (2024) A mini review: How to select electrolyte additives for better Zn anode electrochemistry?, *Energy Storage Materials*, 66, 103227. <https://doi.org/10.1016/j.ensm.2024.103227>
- [12] J. Cao, D. Zhang, X. Zhang, Z. Zeng, J. Qin, Y. Huang (2022) Strategies of regulating Zn<sup>2+</sup> solvation structures for dendrite-free and side reaction-suppressed zinc-ion batteries, *Energy & Environmental Science*, 15(2), 499-528. <https://doi.org/10.1039/D1EE03377H>
- [13] F.W.T. Goh, Z. Liu, T.S.A. Hor, J. Zhang, X. Ge, Y. Zong, A. Yu, W. Khoo (2014) A near-neutral chloride electrolyte for electrically rechargeable zinc-air batteries, *Journal of the Electrochemical Society*, 161(14), A2080. <https://doi.org/10.1149/2.0311414jes>
- [14] Y. Du, Y. Li, B. B. Xu, T. X. Liu, X. Liu, F., Ma, C. Lai (2022) Electrolyte salts and additives regulation enables high performance aqueous zinc ion batteries: a mini review, *Small*, 18(43), 2104640. <https://onlinelibrary.wiley.com/doi/full/10.1002/smll.202104640>
- [15] X. Zhang, J.-P. Hu, N. Fu, W.-B. Zhou, B. Liu, Q. Deng, X.-W. Wu (2022), Comprehensive review on zinc-ion battery anode: challenges and strategies. *InfoMat*, 4(7), 12306. <https://doi.org/10.1002/inf2.12306>

[16] O. Aaboubi, J. Douglade, X. Abenaqui, R. Boumedmed, J. VonHoff (2011). Influence of tartaric acid on zinc electrodeposition from sulphate bath. *Electrochimica Acta*, 56(23), 7885-7889. <https://doi.org/10.1016/j.electacta.2011.05.121>

[17] Y. Geng, L. Pan, Z. Peng, Z. Sun, H. Lin, C. Mao, L. Wang, L. Dai, H. Liu, K. Pan, X. Wu, Q. Zhang, Z. He (2022), Electrolyte additive engineering for aqueous Zn ion batteries. *Energy Storage Materials*, 51, 733-755. <https://doi.org/10.1016/j.ensm.2022.07.017>

[18] J. Gong, J. Ying, X. Jia, R. Su, T. Zhao, H. Jiang (2024) Dendrite-free zinc anode enabled by bifunctional additive coupling electrostatic shielding and zincophilic leveling, *Chemical Engineering Journal*, 480, 148267. <https://doi.org/10.1016/j.cej.2023.148267>

[19] A. Bayaguid, X. Luo, Y. Fu, C. Zhu (2020) Cationic surfactant-type electrolyte additive enables three-dimensional dendrite-free zinc anode for stable zinc-ion batteries, *ACS Energy Letters*, 5(9), 3012-3020. <https://doi.org/10.1021/acsenergylett.0c01792>

[20] Q. Cao, Y. Gao, J. Pu, A. M Elshahawy, C. Guan (2024) Materials and structural design for preferable Zn deposition behavior toward stable Zn anodes, *SmartMat*, 5(1), 1194. <https://doi.org/10.1002/smm.2.1194>

[21] M. C. van Ede, U. Angst (2022) Analysis of polarization curves under mixed activation-diffusion control: an algorithm to minimize human factors. *Corrosion*, 78(11), 1087-1099. <https://doi.org/10.5006/4171>

[22] M. E. McMahon, R. J. Santucci Jr., J. R. Scullya (2019), Advanced chemical stability diagrams to predict the formation of complex zinc compounds in a chloride environment. *RSC advances*, 9(35), 19905-19916. <https://doi.org/10.1039/C9RA00228F>

[23] S. Clark, A. Latz, B. Horstmann (2017) Rational development of neutral aqueous electrolytes for zinc-air batteries, *ChemSusChem*, 10(23), 4735-4747. <https://doi.org/10.1002/cssc.201701468>

[24] B. J. Mhin, S. Lee, S. J. Cho, K. Lee, K. S. Kim (1992)  $Zn(H_2O)^{2+}_6$  is very stable among aqua-Zn (II) ions, *Chemical Physics Letters*, 197(1-2), 77-80. [https://doi.org/10.1016/0009-2614\(92\)86025-D](https://doi.org/10.1016/0009-2614(92)86025-D)

[25] Q. Zong, R. Li, J. Wang, Q. Zhang, A. Pan (2024) Tailoring the whole deposition process from hydrated  $Zn^{2+}$  to  $Zn^0$  for stable and reversible Zn anode, *AngewandteChemie*, 136(41), 202409957. <https://doi.org/10.1002/anie.202409957>

## IZVOD

### UTICAJ TARTARATA NA TALOŽENJE-RASTVARANJE CINKA ZA PRIMENU U BATERIJAMA NA BAZI VODENIH RASTVORA

Cink-jonske baterije (ZIB) su nedavno dobitne značajnu pažnju kao održivo rešenje za skladištenje energije zbog svoje isplativosti i sigurnosti. Uprkos tome što nude visok teoretski kapacitet i nizak redoks potencijal, ZIB se suočavaju sa izazovima kao što su rast dendrita i niske stope iskorišćenja cinka, što ometa njihov učinak. Cilj ove studije je bio da se optimizuje sastav elektrolita kako bi se poboljšale performanse cink elektrode elektrohemski deponovane na bakarnoj podlozi u sistemu cink(II)-NH4Cl. Ispitivan je uticaj koncentracija jona  $Zn^{2+}$  i  $NH_4^+$ , gustine struje i dodatka natrijum-tartarata na morfologiju i ponašanje anodnog materijala tokom ciklusa punjenja i pražnjenja. Rezultati su pokazali da dodatak natrijum tartarata značajno poboljšava elektrohemiske performanse anodnog materijala i smanjuje koroziju u elektrolitu. Nalazi ove studije sugeriraju da bi inženjeriranje elektrolita potencijalno mogao da pruži rešenje za bolje performanse i produženi vek ZIB-a.

**Ključne reči:** Cink-jonske baterije, natrijum tartarat, aditiv, anoda, korozija.

Naučni rad

Rad primljen: 24.12.2024.

Rad prihvaćen: 24.01.2025.

The ORCID Ids of all the authors are as follows:

Aleksandra S. Popović:	<a href="https://orcid.org/0000-0002-4432-0183">https://orcid.org/0000-0002-4432-0183</a>
Dušan Vujošević:	N/A
Milan Milivojević:	N/A
Tomislav Trišović:	<a href="https://orcid.org/0000-0003-2400-5984">https://orcid.org/0000-0003-2400-5984</a>
Lazar Rakočević:	<a href="https://orcid.org/0000-0001-6199-8087">https://orcid.org/0000-0001-6199-8087</a>
Branimir N. Grgur:	<a href="https://orcid.org/0000-0003-4684-9053">https://orcid.org/0000-0003-4684-9053</a>